Change of the Electronic Conductivity of CNTs and Graphene Sheets Caused by Three-dimensional Strain Field

M. Ohnishi*, H. Kawakami*, Y. Suzuki*, K. Suzuki**, and H. Miura**
* Dept. of Nanomechanics, Graduate School of Eng., Tohoku University
6-6-11-716 Aobayama, Aoba-ku, Sendai, 980-8579, Japan, masato@rift.mech.tohoku.ac.jp
** Fracture and Reliability Research Institute, Graduate School of Eng., Tohoku University

ABSTRACT

In this study, the change of the conductivity of carbon nanotubes (CNTs) and graphene nanoribbons (GNRs) under deformation was analyzed by applying a molecular dynamics and the density functional theory (DFT). Various combinations of double-walled CNT structures were modeled for the analysis. The change of the band structure was calculated by changing the amplitude of the applied strain. It was found in some cases that the band structure changes drastically from metallic structure to semiconducting structure, and this result clearly indicated that the electronic conductivity of this multi-walled CNT (MWCNT) decreased significantly in a three-dimensional strain field.

Keywords: carbon nanotube, graphene nanoribbon, strain, conductivity, DFT

1 INTRODUCTION

Recently, physical and chemical properties of CNTs have been investigated by quite a few researchers all over the world in detail, and their unexpected superior characteristics have been made clear theoretically and experimentally. Both the electronic and mechanical properties of CNTs are almost the same as metals and are deformed easily and stable chemically. In addition, their resistivity changes drastically under applied strain, it is possible, therefore to develop a highly sensitive strain sensor [1-3].

Thus, the authors have proposed a new highly sensitive strain sensor using a popular resin in which CNTs are dispersed uniformly [4]. It is easy to make a cheap, flexible and stable sensor by using the CNT-dispersed resin. The measured change rate was 400%/%strain under tensile strain and 150%/%strain under compressive strain, respectively. These values were about a hundred times higher than that of metallic strain gauges. So, the possibility of high sensitivity strain measurement was revealed. However, there was large fluctuation of the measured change rate among test samples. Therefore, it is very important to clarify the mechanism of the change of the resistance of a CNT due to its deformation.

In order to discuss the relationship between the deformation of a CNT and its electronic conductivity, both a molecular dynamics analysis and the DFT calculation were applied. In this study, various combinations of double-walled CNT structures were modeled for the analyses. The change of the resistivity of MWCNTs under uniaxial strain was analyzed by applying DFT. And the change of the band structure of a GNR was also analyzed by applying the DFT.

2 DEFORMATION ANALYSIS OF CNTs

It is well known that the resistance of CNTs changes drastically under strain. Stampfer et al. showed large gauge factors in excess of 2900 [5]. Since the conductivity change is caused by the deformation of the CNT, it is very important to understand the deformation behavior of a CNT under strain. Deformation characteristics of CNTs under axial strain were investigated by molecular dynamics (MD). The simulation cell consisted of a (17,0) CNT with length 100.7 Å and 1632 carbon atoms and the CNT was placed in the middle of the cell. In the simulations, the periodic boundary condition is imposed on three dimensions. The basal surface area was enough large (> 100 Å × 100 Å) that the interaction of CNTs in next cells could be neglected. The height of the cell was equal to the length of the CNT. All simulations were undertaken by using the Tersoff potential of LAMMPS package [6]. NPT (300 K, 1 atm) simulations were firstly performed to acquire the equilibrium state. After this relaxation analysis, it was assumed that a CNT structure was under stress (strain)-free condition. Then, the height of the cell was changed with the velocity of 2.0 m/s for the loading analysis. In this analysis, x and y coordinates of atoms of the CNT at regions of 3 Å from both ends were fixed. Analysis conditions were summarized in Table 1.

Figure 1 shows examples of distributions of C-C bond lengths of the CNT under axial strain. A red line in each figure shows an average value of bond lengths of CNT. Bond lengths varied 1.41 to 1.55 Å in the CNT without strain and its average bond length was 1.46 Å, witch was good

Table 1: Deformation analysis conditions

	Relaxation analysis	Loading analysis
Potential Function	Tersoff	Tersoff
Ensemble	NPT	Volume change
Temperature	300 K	300 K
Time Step	1.0 fs	1.0 fs
Total Step	10,000	1,000,000
Deformation Velocity	-	2.0 m/s

agreement with the experimental value [7]. The average distance increased monotonically as the increase in tensile strain as shown in Fig. 2. Fig. 1(b) shows that there were two distribution types when the value of tensile strain was 10%; small-extended bond lengths extended to 1.50 ± 0.4 Å and large-extended bond lengths extended to 1.64 ± 0.8 Å. The ratio of those bond lengths was about 1.1 in this case. The zigzag CNTs have two types of C-C bonds in terms of the bond direction, (A) C-C bonds not parallel to the tube axis and (B) those parallel to the axis. Therefore, observed different distribution indicates that bond lengths of type B (parallel to the tube axis) extended larger than bond lengths of type A (not parallel to the axis) and consequently six-membered rings in a CNT were distorted under uniaxial tensile strain.

In the case of the compressive strain, the CNT showed simple shrinkage deformation when the amplitude of the applied compressive strain was less than 3% and then, the average bond length decreased monotonically in this compressive strain region. The average bond length, however, increased when the amplitude of the applied compressive strain exceeded 3% (after buckling as shown in Fig. 1(c)). Figure 1(c) shows that the behavior of bond length change around buckling areas and that of other areas are different significantly. Around buckling area, C-C bond lengths had larger width of distribution than those of other areas. Thus, buckling deformation of CNTs causes a very complicated strain distribution in the tube. Therefore, the clarification of the change mechanism of the electronic state of CNTs is very important to develop a strain sensor or electronic devices based on CNTs.

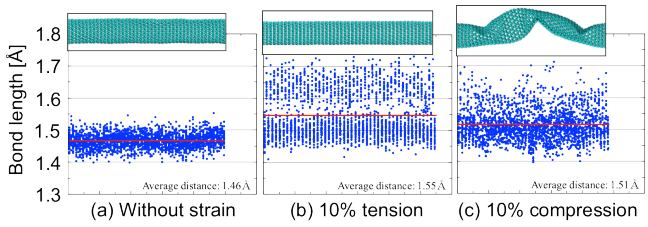

Figure 1: Estimated deformation of a (17,0) CNT under uniaxial strain

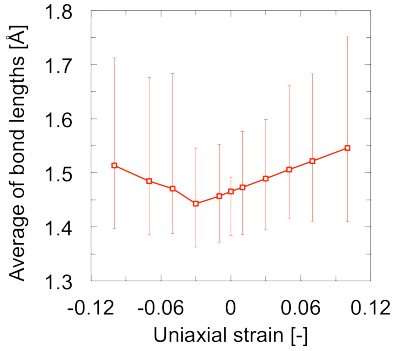

Figure 2: Change of the average of bond lengths of (17,0) CNT under uniaxial strain

3 CHANGE OF ELECTRONIC STATE OF CNTs AND GNRs UNDER STRAIN

In the previous section, we described that the ratio of bond lengths changes significantly depending on the C-C bond direction when the uniaxial tensile strain is applied and that the buckling deformation leads the complicated deformed CNT structure when the compressive strain is applied to a CNT. In this study, we analyzed the effect of the distortion of six-membered rings on the local electronic state of a CNT and the effect of the change of the curvature (or the radial strain) on the electronic state of GNRs and CNTs in order to estimate the local conductivity change caused by the tensile and compressive strain, respectively.

To understand the effect of the uniform uniaxial strain, the band gap change of CNTs under uniaxial strain was calculated by using π orbital tight-binding approximation [8]. We used the hopping integral, which decreased exponentially with bond length in this analysis [9]. Figure 3 shows an example of the band gap change of a single-walled (17,0) CNT under uniform uniaxial strain. We applied uniaxial strain of -10 to 20% to the CNT. In this figure, the amplitude of uniaxial strain and the ratio of b/a, where *a* is the bond length of type A and *b* is the bond length of type B, are shown in major and minor axis, respectively. The bond length ratio $b/a = 1$ indicates the undistorted six-membered ring and larger value of $|b/a - 1|$ indicates the larger distortion of six-membered ring. The values of *a* and *b* at 0% strain are 1.420 Å and 1.418 Å, respectively.

When the ratio of the bond lengths b/a was 1.00 to 1.10, the band gap decreased from 0.3 to 0.0 eV in the range of $b/a = 1.00$ to 1.03 and increased from 0.0 to 0.5 eV in the range of $b/a = 1.03$ to 1.10. Because the ratio of the bond lengths b/a changed drastically, at least 1.0 to 1.1, as clarified at the previous section, the large and complicated change of the conductivity occurs in the CNT caused by the applied strain.

Since buckling deformation causes the complicated distortion of six-membered rings as mentioned in the previous section and then, the increase in the curvature around buckling areas leads to the orbital hybridization, which changes the electronic state of CNT complicatedly, it is difficult to estimate the electronic state by using tight-

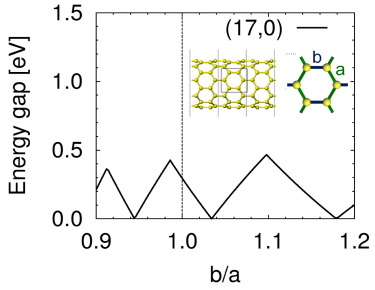

Figure 3: Effect of the ratio change of the bond length parallel to the tube axis to that not parallel to the axis to the band gap of (17,0) CNT

binding approximation. We, therefore, applied the DFT to discuss the effect of local buckling of a CNT on its electronic band structure. The change of the electronic band structure of the deformed GNRs and CNTs were analyzed by using Accelrys' DFT-code DMol^3 [10], the DFT based on the generalized gradient approximation (GGA) of PW91 [11]. The total energy was converged to within 0.5 meV with a Monkhorst-Pack *k*-point mesh of $1 \times 1 \times 50$. Vacuum separations along both *a* and *b* axis were more than 50 Å, which was enough large to neglect the interaction of next cells. The length along *c* axis was equal to the transverse vector of GNRs and CNTs.

Firstly, we modeled GNRs which was applied a longitudinal strain and a curvature as shown in Fig. 4. We fixed the nearest-neighbor bond lengths when the curvature is applied for excluding other effects except to orbital hybridization caused by orbital hybridization on the electronic state of GNR.

Figure 4 shows an example of the change of the band gap of GNRs under strain. In this analysis, we used an armchair GNRs (AGNR) with width N=10, a hydrogen terminated unzipped (5,0) CNTs. The radius of the original (5,0) CNT is 1.96 Å, which corresponds a curvature of 0.51 Å^{-1}. The amplitude of the applied longitudinal strain and that of the curvature were varied -5% to 30% and 0.00 to 0.45 Å, respectively. The electronic property of the AGNR, which has a band gap of 1.1 eV in the original state, changed to metallic state at 10% tensile strain when the longitudinal strain was applied. When the curvature was applied to the semiconducting AGNRs with different longitudinal strain, band gap values decreased exponentially around the applied curvature of 0.3 Å^{-1}. Figure 5 showed an example of the change of the electronic band structure of the AGNR under applied curvature when the longitudinal strain was fixed 0%. When the amplitude of the applied curvature was less than 0.3 Å^{-1}, the third and fourth excitation energies (blue and pink) decreased as the increase in curvature although dispersions of the first and the second excitation energies (red and green) did not change significantly. Once the curvature reached 0.3 Å^{-1} and orbital hybridization occurred, the first and the second excitation energies decreased drastically. This indicates that the first and the second band energies, which are dominant on the electronic conductivity, do not change significantly when the amplitude of the applied curvature is small. They, however, decrease drastically once hybridization occurred, which causes the decrease in band gap of the GNR.

In order to discuss the effect of local buckling of a CNT on its electronic band structure, the radial strain is applied to a CNT. The change of the electronic band structure of the deformed CNT was calculated by using the DFT.

We analyzed electronic states of (9,0) CNTs under strain, which had a radius of 3.5 Å corresponding a curvature of 0.28 Å in the original state. An axial and a radial strain were applied to the CNTs and the change of their electronic states was analyzed. During the radial strain loading, the shape of the cross section was maintained as an ellipse in this analysis. The semi-major axis of the ellipse can be written R= (1 + ε_R) R_0, wher ε_R is the radial strain and ε_0 is the radius of the original CNT, 3.5 Å. The amplitudes of the axial and the radial strains were varied -5 to 20 % and 0 to 30%, respectively.

Figure 6 summarizes the effect of the axial strain on the electronic band gap of the CNT under the radial strain. When the radial strain is zero, the CNT has a small band gap. However, band gap increases clearly with increase of the applied tensile strain. In addition, the band gap also appears when the radial strain is applied to the CNT. The amplitude of the developed band gap is a strong function of both the radial and axial strain. Figure 7 also summarizes the effect of the radial strain on the band gap of the (9, 0) CNT. In this

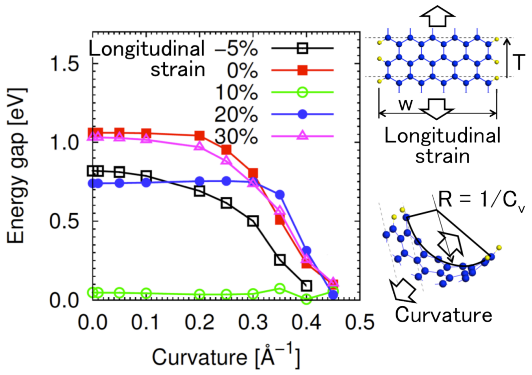

Figure 4: Analysis model and change of band gap of AGNR (N=10) caused by applied curvature (axial strain: 0%)

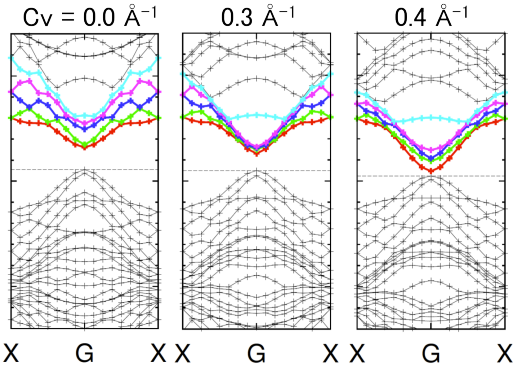

Figure 5: Change of electronic band structure of AGNR (N=10) caused by applied curvature (longitudinal strain: 0%)

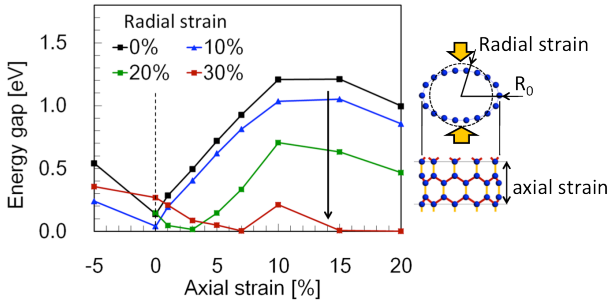

Figure 6: Analysis model and effect of axial and radial strain on the band gap of a (9, 0) CNT under radial strain

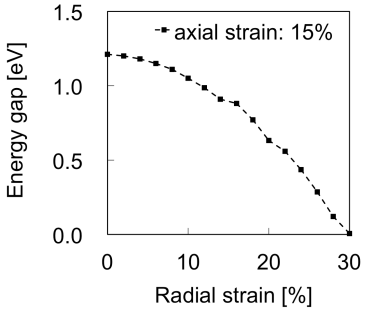

Figure 7: Effect of radial strain on the electronic band structure of a (9, 0) CNT under the axial strain at 15%

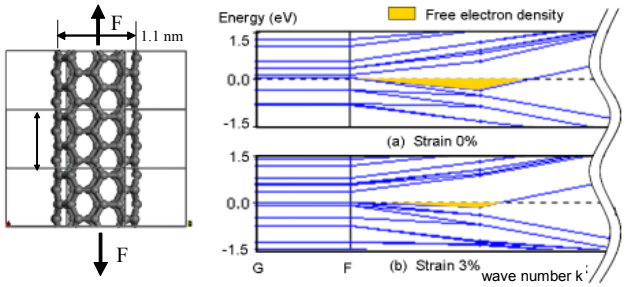

Figure 8: Change of the band structure a (14,0)-(6,0) MWCNT under a uniaxial strain

figure, the axial tensile strain is fixed at 15%. It was found that the band gap decreases monotonically with increase of the radial strain. Even under the tensile strain at 15%, the CNT recovers from semiconducting characteristic to metallic characteristic when the radial strain is about 30%. These results clearly indicate that the electronic band structure, and thus, the electronic conductivity of the deformed CNT varies drastically and complicatedly depending on the three-dimensional strain filled in it.

Finally, we also modeled various combinations of double-walled CNT structures were modeled for the analysis. An example of a (14,0)-(6,0) MWCNT is shown in Fig. 8. The outer tube is semiconducting and the inner tube is metallic. The length of the tube was varied by considering the uniaxial strain. An example of the calculated result of the band structure (in the vicinity of Fermi level) is also shown in this figure. Since the band cuts across the Fermi level (dotted line in the figure), this MWCNT is metallic. We calculated again the band structure under the uniaxial tensile strain of 3%. It was found that the band structure changes drastically, and this result clearly indicates that the electronic conductivity of this MWCNT decreases significantly under tensile strain. It was found that further application of the strain made a band gap in the band structure. This result indicates that the metallic CNT changes a semiconducting CNT due to the applied strain.

Next issue to be solved is to make clear the change of the resistance of the deformed CNT quantitatively based on the estimated distribution of the local electronic band structure in the deformed CNT.

4 CONCLUSIONS

In this study, the change of the configuration structure and the electronic state of CNTs and GNRs under deformation was analyzed by applying a molecular dynamics, a tight-binding approximation and the DFT calculation. Since the conductivity change is caused by the deformation of the CNT, deformation characteristics of CNTs under axial strain were investigated. We found that six-membered rings in a CNT were distorted under both uniaxial tensile and compressive strain. Especially, buckling deformation of CNTs causes the change of the very complicated strain distribution and the increase in the local curvature in a tube. To understand the effect of the uniform uniaxial strain, the band gap change of CNTs under uniaxial strain was calculated by using a tight-binding approximation. The bond length ratio *b/a* was found to be a dominant factor which changes the electronic state of CNTs under strain. Since the CNT consists of a periodical structure of a six-membered carbon ring, the change of the band structure of a GNR caused by the distortion of the six-membered ring structure was analyzed. In order to discuss the effect of local buckling of a CNT on its electronic band structure, the radial strain is applied to a CNT. We clarified that the electronic band structure of the deformed CNT varies drastically and complicatedly depending on the three-dimensional strain filled in it. Therefore, the electronic conductivity of a GNR and thus, a CNT was found to be mainly dominated by the fluctuation of the distance between the nearest carbons.

REFERENCES

[1] Prasad Dharap, Zhiling Li, Satish Nagarajaiah1and E V Barrera, Nanotechnology, Vol. 15, pp. 379-382 (2004).

[2] Inpil Kang, Mark J Schulz, Jay H Kim, Vesselin Shanov, and Donglu Shi, Smart Material Structures, Vol. 15, pp. 737-748, (2006).

[3] W. Zhang, J. Suhr, and N. Koratkar, Nanoscience and Nanotechnology, Vol. 6, pp. 960-964, (2006).

[4] K. Suzuki, Y. Suzuki, Y. Ohashi, M. Ohnishi, H. Miura, Abstract of Solid State Devices and Materials (2011).

[5] C. Stampfer, A. Jungen, R. Linderman, D. Obergfell, S. Roth, and C. Hierold, Nano Lett. 6, 1449 (2006).

[6] Plimpton (1995) J. Comp. Phys. 117, 1-19. (http://lammps.sandia.gov).

[7] T. W. Odom, J. L. Huang, P. Kim, and C. M. Lieber, Nature, 391, 62 (1998).

[8] L. Yang, M. P. Anantram, J. Han, and J. P. Lu, Phys. Rev. B 60, 13874-13878 (1999).

[9] V. M. Pereira, A. H. C. Neto, and N. M. R. Peres, Phys. Rev. B 80, 045401 (2009).

[10] B. Delley, J. Chem. Phys. 92, 508 (1990); J. Phys. Chem. 100, 6107 (1996).

[11] J. P. Perdew, J. A. Chevary, S. H. Vosko, K. A. Jackson, M. R. Pederson, D. J. Singh, and C. Fiolhais, Phys. Rev. B 46, 6671 (1992); 48, 4978 (1993).